An exact homogenization method in heat conduction

Gal Shmuel[i]
Department of Mechanical Engineering, Technion-Israel Institute of Technology, Israel
John R. Willis[ii]
Department of Applied Mathematics and Theoretical Physics,
Centre for Mathematical Sciences, University of Cambridge
Wilberforce Road, Cambridge CB3 0WA, U.K.

Abstract

We determine the macroscopic features of thermal transport in heterogeneous conductors by generalizing an exact, source-driven homogenization method originally developed for waves. The formulation accommodates random or periodic media of finite or infinite extent, with or without pores. Our homogenization shows that the effective heat flux and entropy are spatiotemporally nonlocal functions of both the effective temperature and its gradient, and that the emergent bianisotropic cross-couplings form an adjoint pair when the microscopic relations are self-adjoint. A spatially local approximation highlights how the homogenized diffusion equation can become hyperbolic due to temporal nonlocality, and that the medium's thermal impedance can become direction-dependent as captured by the bianisotropic terms. In addition, we develop a retrieval method for one-dimensional deterministic composites, whose results reinforce our conclusions.

1 Introduction

The transport of energy strongly depends on the inhomogeneities of the medium through which it propagates. Here, we determine the macroscopic features of thermal energy transport in heterogeneous conductive media by developing a homogenization method that relates appropriately averaged fields through the effective properties of a fictitious homogeneous medium. Our method reveals effective behavior that differs fundamentally from the microscopic one. Notably, our method rigorously identifies macroscopic cross-couplings between thermodynamic fields that are microscopically independent; and, under certain conditions, predicts finite speed of heat propagation, as detailed in subsequent sections.

Homogenization methods provide effective models aimed at capturing the macroscopic behavior of heterogeneous media [1, 2], often using asymptotic series expansions based on some scale separation assumptions [3–5]. In contrast with these asymptotic methods, Willis introduced a method for elastic waves that is applicable to all wavelengths and frequencies [5–10], revealing macroscopic transport phenomena absent at the microscopic scale. Of particular relevance are the macroscopic cross-coupling between stress and velocity, and between linear momentum and strain, now known as the Willis couplings [11–13].

[i] meshmuel@technion.ac.il
[ii] jrw1005@cam.ac.uk

Since Willis' method contains no approximations, it is regarded as exact [10]; and in fact its asymptotic expansion coincides with results from asymptotic homogenization [5].

The applicability of the framework developed by Willis extends beyond elastic transport. In analogy with Willis tensors in elastodynamics, applying this framework to electromagnetic composites reveals the emergence of effective bianisotropic (magnetoelectric) tensor terms, even in centrosymmetric crystals without bianisotropic constituents [8]. Pernas-Salomón and Shmuel [14] extended the framework to dynamics of piezoelectric composites, which exhibit inherent cross-couplings of mechanical and electric fields. Their unified theory revealed a macroscopic cross-coupling between the electric field and linear momentum density, termed the electromomentum coupling, analogous to the Willis coupling in elastodynamics [15–18].

Building on Willis' homogenization framework, here we develop an exact homogenization method for heat conduction in a general, time-independent, three-dimensional random medium of finite or infinite extent, with or without pores. We provide a detailed derivation of the method, noting that a summary of the conclusions of our exact approach is given in a companion paper [19]. Guided by these conclusions, we also carried out a heuristic homogenization of a subwavelength element based on its scattering properties in Ref. [19]. Here, we also elaborate on the derivation of this heuristic method.

Before presenting our formulations and numerics, we summarize prior work on thermal Willis couplings and explain how our analysis advances the field. The first theoretical observation was by Torrent et al. [20], who analyzed a one-dimensional medium whose properties are periodically modulated both in space and time. Such time-dependent modulation is challenging and has yet to be realized in practice. The infinite periodic nature of the problem enabled Torrent et al. to employ Floquet–Bloch homogenization [11] and obtain an effective convection-diffusion equation with a coefficient analogous to the Willis coupling. In contrast with our conclusions, the thermal Willis coupling that they identify vanishes in the absence of time-modulation, and the effective differential equation has no second time derivative. Xu et al. [21, 22] likewise employed Floquet–Bloch homogenization of a medium with periodically spatiotemporal modulated properties. Their resultant governing equation differs from its counterpart in Ref. [20], and includes a single thermal Willis coupling. These differences stem from the nonlocal nature of the macroscopic response, which makes the homogenized description non-unique. We elaborate on this issue in Sec. 2, and resolve it using a source-driven homogenization approach [8, 13, 14, 23, 24].

We recognize the entropy-temperature relationship as a second constitutive relation alongside Fourier's law, enabling us to identify two bianisotropic (cross-coupling) terms rather than one. This aspect is absent in the homogenization schemes of Refs. [20–22], the last of which explicitly states that diffusion systems admit a single constitutive relation.

We recall that our method is applicable not only to infinite periodic media but also to random, possibly finite media. To treat randomness in the medium's composition, we model its physical properties as properties that vary not only with position but also within a sample space equipped with a probability measure. The effective fields are accordingly defined by the ensemble mean; the formulation here is more general than the one introduced in our companion paper, in that it allows for voids in the medium by

employing a weighted mean in the averaging process [8, 25, 26]. Our formulation treats a periodic medium as a particular case of a random medium by considering the corner of its periodic cell as a uniformly distributed random variable. A key ingredient in the method is the Green's function of the medium, which accounts for boundary conditions of a possibly finite medium. [8, 25, 26].

Collectively, our homogenization principles yield a unique class of nonlocal effective relations that remain self-adjoint when the microscopic relations are self-adjoint. In electrodynamics and (electro-)elastodynamics, the effective differential equation preserves the hyperbolic character of the microscopic equation. Here, by contrast, the effective equation includes both a second-order time derivative and a mixed space-time derivative, and, under certain conditions, is hyperbolic, predicting finite-speed heat propagation. While conclusive experimental evidence supporting this prediction is still lacking, we note that the indications reported to date involve heterogeneous materials [27–29] . This inevitable outcome of our homogenization procedure coincides with the objective of many phenomenological models, most prominently Cattaneo's model [30, 31].

Our results are presented in the following order. First, we explain in Section 2 the origins of non-uniqueness in effective models and our approach to resolving it. In Section 3 we review the equations for heat conduction in randomly heterogeneous materials and then derive our exact homogenization method in Section 4. The main conclusions drawn from the resultant effective description are presented in Section 5. These conclusions are reinforced by results of a retrieval method for the effective properties of one-dimensional deterministic composites, which we develop in Section 6. Corresponding numerical calculations appear in Section 7. We conclude this paper with a summary of our main results in Section 8.

This work is dedicated to the memory of our dear colleague, Dr. Sarah Benchabane, and her husband Oliver and son Aaron.

2 Nonlocality and non-uniqueness of effective constitutive relations

This Section concisely explains the source of the difference between the homogenized equations of Torrent et al. [20], Xu et al. [21, 22] and our equations. The explanation mirrors earlier discussions in other contexts [8, 11, 13, 15], restated here for heat conduction.

In the Floquet–Bloch domain, spatiotemporal derivatives become multipliers in the transform variables; dependence of the effective relations on these multipliers reflects nonlocality in space and time. Since these variables commute with averaging, an ambiguity arises in defining the effective kinematic state variables. For heat conduction, this means that the effective temperature and the effective temperature gradient—both derived from the same potential—are no longer algebraically independent. Thus, in the absence of sources, Floquet–Bloch analysis yields only a dispersion relation, leaving open the attribution of contributions arising from heat flux and free energy. This ambiguity is removed if a heat source is admitted but even then the constitutive relations cannot be defined uniquely, owing to the linear dependence between temperature and temperature gradient. There exists, instead, an equivalence class of effective relations. To

identify a unique representative of this class, we introduce a residual temperature-gradient field acting as a source, analogous to the eigenstrain in Ref. [8]. In electromagnetics and (electro-)elastodynamics, works show that this prescription allows for the proper identification of cross-couplings and yields constitutive properties that satisfy physical constraints such as reciprocity and energy conservation [13, 16, 17, 32]. By contrast, these constraints are violated when the cross-coupling terms are erroneously lumped into the direct couplings.

A second non-uniqueness arises when transforming back to the time domain, since the transform time variable can be identified either as part of the kernel or as part of an effective kinematic rate field. In elastodynamics, this translates to two classes of constitutive relations—one depending on effective velocity and the other on effective acceleration [12, 33]. Here, the analogous choice is between effective temperature and effective temperature rate.

3 Heat conduction in random composites

3.1 Governing equations

Consider a randomly inhomogeneous conducting material occupying a fixed domain Ω. As such, its thermal conductivity $\boldsymbol{\kappa}$ and specific heat c are not only functions of the spatial coordinate $\mathbf{x}$, but also of some parameter, say α, in a sample space $\mathcal{A}$ endowed with a probability measure μ. A part $\partial\Omega_\theta$ of its boundary $\partial\Omega$ is subjected to a prescribed non-random (sure) temperature increment $\theta^0(\mathbf{x},t)$ for $t>0$. The complementary part $\partial\Omega_q$ is subjected to an outward heat flux $\mathbf{q}\cdot\mathbf{n}=w^{(1)}(\mathbf{x},\alpha)q^0(\mathbf{x},t)$, where $\mathbf{q}$ is the heat flux, $\mathbf{n}$ is the outward normal to $\partial\Omega$, $q^0(\mathbf{x},t)$ is sure but $w^{(1)}(\mathbf{x},\alpha)$ represents the values on $\partial\Omega_q$ of a random field $w^{(1)}(\mathbf{x},\alpha)\geq 0$, defined over (the closure of) Ω, with ensemble mean

$$\left\langle w^{(1)}\right\rangle=\int_{\mathcal{A}} w^{(1)}(\mathbf{x},\alpha)\mathrm{d}\mu=1. \tag{3.1}$$

The body is also subjected to a prescribed heat input $r(\mathbf{x},t,\alpha)=w^{(1)}(\mathbf{x},\alpha)r^0(\mathbf{x},t)$, where r^0 is sure. The motivation for including $w^{(1)}$ in the formulation is that the material could for example be porous and $w^{(1)}$ could be chosen to be zero within the pores but there is no need to be so specific in the formulation. The temperature increment $\theta(\mathbf{x},t,\alpha)$ is prescribed to be zero throughout Ω when $t=0$. It is useful to apply the Laplace transform with respect to time, by which functions in the transform domain depend on s, and time derivatives are replaced by multiplication by s. The case of time-harmonic sources is obtained by taking $s=i\omega$.

The temperature, now represented as $\theta_{\mathrm{R}}+\theta(\mathbf{x},s,\alpha)$[iii], where θ_{R} is the (uniform) reference temperature, is governed by the linearized equation of energy conservation

$$-\nabla\cdot\mathbf{q}+r=s\theta_{\mathrm{R}}\eta, \tag{3.2}$$

[iii] With abuse of notation, we use the same symbols for functions and their Laplace transform.

where η is increment of entropy. The kinetic fields $\mathbf{q}$ and η are functions of the kinematic fields $\nabla\theta$ and θ via the linear, time-invariant, and local constitutive equations

$$-\mathbf{q} = \boldsymbol{\kappa}(\nabla\theta - \boldsymbol{\zeta}), \quad \theta_{\mathrm{R}}\eta = c(\theta - \varphi), \tag{3.3}$$

where $\boldsymbol{\zeta}$ is a purely artificial residual thermal gradient, analogous to the artificial magnetic polarization for electrodynamics, or the strain polarization introduced by Willis [8, 9, 34], for the purpose of making a unique choice from the equivalence class of effective constitutive tensors. The additional residual field φ is included just for symmetry; either one of $\boldsymbol{\zeta}$ and φ could be set to zero.

3.2 Symbolic matrix notation

We recast the problem of heat conduction in a symbolic matrix form, which will be useful in the subsequent homogenization scheme. First, we rewrite the energy equation as

$$\mathsf{D}^{\mathsf{T}}\mathsf{h} = -\mathsf{f}, \tag{3.4}$$

where $\mathsf{D}^{\mathsf{T}} = \begin{pmatrix} \nabla\cdot & -s \end{pmatrix}$ is a row vector representing a differential operator acting on the column vector of kinetic fields $\mathsf{h} = \begin{pmatrix} -\mathbf{q} \\ \theta_{\mathrm{R}}\eta \end{pmatrix}$, and $\mathsf{f} = r$. The structure in Eq. (3.4) corresponds to the structure introduced by Willis [8] for electromagnetics and elastodynamics, when projected onto a lower-order tensor space. For example, in elastodynamics f represents a (body-force density) vector field rather than a scalar field,the first component of h is a second-order (stress) tensor field rather than a vector field, and so on[iv].

Next, we recast the constitutive equations in the form

$$\mathsf{h} = \mathsf{L}\left(\mathsf{b} - \mathsf{m}\right), \tag{3.5}$$

where

$$\mathsf{L} = \begin{pmatrix} \boldsymbol{\kappa} & \mathbf{0} \\ \mathbf{0}^{\mathsf{T}} & c \end{pmatrix}, \quad \mathsf{m} = \begin{pmatrix} \boldsymbol{\zeta} \\ \varphi \end{pmatrix}, \tag{3.6}$$

and the kinematic vector b is obtained by applying the differential operator $\mathsf{B} = \begin{pmatrix} \nabla \\ 1 \end{pmatrix}$ to the potential $\mathsf{w} = \theta$[v]. While the operator B defined in Refs. [8, 14] includes time differentiation, here it only contains a spatial gradient; this results in a parabolic governing equation.

Combining Eqs. (3.4) and (3.5) reads

$$\mathsf{D}^{\mathsf{T}}\mathsf{L}\left(\mathsf{B}\mathsf{w} - \mathsf{m}\right) = -\mathsf{f}. \tag{3.7}$$

[iv] Conversely, the structure of Pernas-Salomón and Shmuel [14] generalizes Willis' result [8], by accounting for additional differential operations and field variables present in the electroelastic problem.

[v] The purpose of these apparently redundant definitions (such as $\mathsf{f} = r$ earlier) is to link this structure to the general structure in Ref. [14].

3.3 Macroscopic formulation

The next objective is to develop a macroscopic formulation using meaningful effective field variables and constitutive relations. To this end, we define the effective fields by ensemble averaging [1, 8], as in Eq. (3.1), which identically satisfy the ensemble average of Eq. (3.7)

$$\mathsf{D}^{\mathsf{T}} \langle \mathsf{h} \rangle = -\mathsf{f}, \tag{3.8}$$

where $\mathsf{f} = \langle \mathsf{f} \rangle$ since r is sure. The outstanding problem is to relate $\langle \mathsf{h} \rangle$ to a weighted mean $\left\langle w^{(2)} \mathsf{b} \right\rangle$, where $w^{(2)}$ is positive and $\left\langle w^{(2)} \right\rangle = 1$. This symbolic notation means that the effective constitutive relations relate the ensemble means $\langle \mathbf{q} \rangle$, $\langle \eta \rangle$ to a weighted mean of temperature $\left\langle w^{(2)} \theta \right\rangle$ and its gradient. We will provide an exact formula showing that these relations are nonlocal in space and time and contain bianisotropic terms, even without modulating $\boldsymbol{\kappa}$ and c in time.

4 The exact homogenization method

Our scheme uses the Green's function of the problem and its adjoint to obtain a useful expression for $\left\langle w^{(2)} \mathsf{b} \right\rangle$ and in turn for $\langle \mathsf{h} \rangle$. With the notation in Sec. 3.2, the equation for $\mathsf{G}(\mathbf{x}, \mathbf{x}')$ is

$$\mathsf{D}^{\mathsf{T}} \mathsf{L} \left(\mathsf{B} \mathsf{G} - \mathsf{m} \right) = -\delta \left(\mathbf{x} - \mathbf{x}' \right), \tag{4.1}$$

where δ is the Dirac delta. To define the adjoint Green's function, we use Green's identity

$$\left(\mathcal{M} \left\{ \mathsf{w} \right\}, \mathsf{v} \right)_\Omega - \left(\mathsf{w}, \mathcal{M}^\dagger \left\{ \mathsf{v} \right\} \right)_\Omega = \text{boundary terms}, \tag{4.2}$$

where $\mathcal{M}$ denotes the operator acting on w as defined by Eq. (3.7), $\mathcal{M}^\dagger$ is the formal adjoint with respect to the bilinear pairing $(a, b)_\Omega = \int_\Omega a(\mathbf{x}, s) \cdot b(\mathbf{x}, s) \mathrm{d}\mathbf{x}$, right-hand side in Eq. (4.2) stands for boundary terms resulting from the surface integral of the bilinear function of w, v and their derivatives. Working this out yields

$$\mathsf{B}^\dagger \mathsf{L}^{\mathsf{T}} (\mathsf{D}^{\mathsf{T}})^\dagger \mathsf{G}^\dagger (\mathbf{x}, \mathbf{x}') = -\delta \left(\mathbf{x} - \mathbf{x}' \right), \tag{4.3}$$

where

$$\mathsf{D}^\dagger = \begin{pmatrix} -\nabla \cdot \\ -s \end{pmatrix}, \quad \mathsf{L}^\dagger = \mathsf{L}^{\mathsf{T}}, \quad \mathsf{B}^\dagger = \begin{pmatrix} -\nabla \\ 1 \end{pmatrix}, \tag{4.4}$$

where $\mathsf{G}^\dagger$ is subjected to $\mathsf{G}^\dagger = \mathsf{0}$ at $\partial\Omega_\theta$ where θ is prescribed and to $\left(\boldsymbol{\kappa}^\dagger \cdot \nabla \mathsf{G} \right) \cdot \mathbf{n} = \mathsf{0}$ at $\partial\Omega_q$ where $\mathbf{q} \cdot \mathbf{n}$ is prescribed. Following a standard procedure, the Green's identity implies the symmetry $\mathsf{G}^\dagger (\mathbf{x}, \mathbf{x}') = \mathsf{G} (\mathbf{x}', \mathbf{x})$.

To derive the effective relations, we first take the product of Eq. (3.7) and $\mathsf{G}^\dagger(\mathbf{x},\mathbf{x}')$, from which we subtract the product of Eq. (4.3) and $\mathsf{w}(\mathbf{x})$ and employ the sifting property of the Dirac delta to obtain

$$\mathsf{w}(\mathbf{x}') = \int_\Omega \mathsf{G}^\dagger \mathsf{f} \mathrm{d}\mathbf{x} + \int_\Omega \mathsf{D}^\mathsf{T} \mathsf{L} \left(\mathsf{B}\mathsf{w} - \mathsf{m}\right) \mathsf{G}^\dagger \mathrm{d}\mathbf{x} - \int_\Omega (\mathsf{D}^\dagger)^\mathsf{T} \mathsf{L}^\dagger \mathsf{B}^\dagger \mathsf{G}^\dagger \mathsf{w} \mathrm{d}\mathbf{x}. \tag{4.5}$$

Using the divergence theorem, integration by parts and the boundary conditions, we arrive at

$$\mathsf{w}(\mathbf{x}') = \int_\Omega \mathsf{G}^\dagger \mathsf{f} \mathrm{d}\mathbf{x} + \int_\Omega (\mathsf{D}^\dagger)^\mathsf{T} \mathsf{G}^\dagger \mathsf{L}^\dagger \mathsf{m} \mathrm{d}\mathbf{x} - \int_{\partial\Omega} \mathsf{G}^\dagger q^0 \mathrm{d}a\mathrm{d}a - \int_{\partial\Omega_\theta} \theta^0 \boldsymbol{\kappa}^\dagger \nabla \mathsf{G}^\dagger \mathbf{n} \mathrm{d}a. \tag{4.6}$$

With a view towards calculating a weighted mean of $\theta(\mathbf{x}')$, $\mathsf{w}(\mathbf{x})$ can be replaced by $\left\langle w^{(2)} \mathsf{w} \right\rangle$ in the surface integral, because θ is prescribed and sure on $\partial\Omega_\theta$ and makes zero contribution over $\partial\Omega_q$ owing to the homogeneous boundary condition satisfied by $\mathsf{G}^\dagger$. Having made that replacement, this part of the surface integral can be transformed back to an integral over Ω, to yield

$$\langle \theta(\mathbf{x}') \rangle = \left\langle w^{(2)} \theta \right\rangle (\mathbf{x}') + \int_\Omega \mathsf{G}^\dagger \mathsf{f} \mathrm{d}\mathbf{x} - \int_{\partial\Omega} \mathsf{G}^\dagger \mathbf{q} \cdot \mathbf{n} \mathrm{d}a - \int_\Omega (\mathsf{D}^\dagger)^\mathsf{T} \mathsf{G}^\dagger \mathsf{L} (\mathsf{B} \left\langle w^{(2)} \mathsf{w} \right\rangle - \mathsf{m}) \mathrm{d}\mathbf{x}. \tag{4.7}$$

It is convenient now to employ a compact notation with which Eq. (4.7) reads

$$\langle \mathsf{w} \rangle = \left\langle w^{(2)} \mathsf{w} \right\rangle + \mathsf{G}\{w^{(1)}(r^0, -q^0)\} + ((\mathsf{D}^\mathsf{T})^\dagger \mathsf{G}^\dagger)^\dagger \mathsf{L} (\mathsf{B} \left\langle w^{(2)} \mathsf{w} \right\rangle - \mathsf{m}), \tag{4.8}$$

where the integral operator $((\mathsf{D}^\mathsf{T})^\dagger \mathsf{G}^\dagger)^\dagger$ has kernel

$$((\mathsf{D}^\mathsf{T})^\dagger \mathsf{G}^\dagger)^\dagger (\mathbf{x}', \mathbf{x}) = -(\mathsf{D}^\mathsf{T} \mathsf{G}^\dagger)(\mathbf{x}, \mathbf{x}'), \tag{4.9}$$

and

$$\mathsf{G}\{f, g\}(\mathbf{x}') = \int_\Omega \mathsf{G}(\mathbf{x}', \mathbf{x}) f(\mathbf{x}) \mathrm{d}\mathbf{x} + \int_{\partial\Omega_q} \mathsf{G}(\mathbf{x}', \mathbf{x}) g(\mathbf{x}) \mathrm{d}a. \tag{4.10}$$

Multiplying Eq. (4.8) by $w^{(2)}$ and ensemble averaging gives

$$\left\langle w^{(2)} \mathsf{G} w^{(1)} \right\rangle \{r^0, -q^0\} = - \left\langle w^{(2)} ((\mathsf{D}^\mathsf{T})^\dagger \mathsf{G}^\dagger)^\dagger \mathsf{L} \right\rangle (\mathsf{B} \left\langle w^{(2)} \mathsf{w} \right\rangle - \mathsf{m}). \tag{4.11}$$

Hence, so long as $\left\langle w^{(2)} \mathsf{G} w^{(1)} \right\rangle$ is invertible,

$$\{r^0, -q^0\} = - \left\langle w^{(2)} \mathsf{G} w^{(1)} \right\rangle^{-1} \left\langle w^{(2)} ((\mathsf{D}^\mathsf{T})^\dagger \mathsf{G}^\dagger)^\dagger \mathsf{L} \right\rangle (\mathsf{B} \left\langle w^{(2)} \mathsf{w} \right\rangle - \mathsf{m}). \tag{4.12}$$

Substituting this expression back into Eq. (4.8) explicitly relates w to $\left\langle w^{(2)} \mathsf{w} \right\rangle$, i.e., $\theta(\mathbf{x}')$ to $\left\langle w^{(2)} \theta \right\rangle (\mathbf{x}')$. We substitute this key result into the constitutive equations and ensemble average to obtain the effective constitutive relations

$$\langle \mathsf{h} \rangle = \tilde{\mathsf{L}} (\left\langle w^{(2)} \mathsf{B} \mathsf{w} \right\rangle - \mathsf{m}) =: \begin{pmatrix} \tilde{\boldsymbol{\kappa}} & \tilde{\boldsymbol{\chi}} \\ \tilde{\boldsymbol{\xi}} & \tilde{c} \end{pmatrix} (\left\langle w^{(2)} \mathsf{B} \mathsf{w} \right\rangle - \mathsf{m}), \tag{4.13}$$

where

$$\tilde{\mathsf{L}} = \langle \mathsf{L} \rangle - \left\langle \mathsf{LBG} w^{(1)} \right\rangle \left\langle w^{(2)} \mathsf{G} w^{(1)} \right\rangle^{-1} \left\langle w^{(2)} ((\mathsf{D}^{\mathsf{T}})^{\dagger} \mathsf{G}^{\dagger})^{\dagger} \mathsf{L} \right\rangle + \left\langle \mathsf{LB} ((\mathsf{D}^{\mathsf{T}})^{\dagger} \mathsf{G}^{\dagger})^{\dagger} \mathsf{L} \right\rangle . \tag{4.14}$$

In suffix notation, the kernels of the integral operators are

$$\begin{aligned}
\tilde{\kappa}_{ij}(\mathbf{x}, \mathbf{x}') &= \langle \kappa_{ij}(\mathbf{x}) \rangle \\
&\quad + \int_{\Omega} \langle \kappa_{ik}(\mathbf{x}) \partial_{x_k} G(\mathbf{x}, \mathbf{y}) w^{(1)}(\mathbf{y}) \rangle \mathrm{d}\mathbf{y} \int_{\Omega} \langle w^{(2)} G w^{(1)} \rangle^{-1}(\mathbf{y}, \mathbf{z}) \langle w^{(2)}(\mathbf{z}) \{ \partial_{x'_\ell} G(\mathbf{z}, \mathbf{x}') \} \kappa_{\ell j}(\mathbf{x}') \rangle \mathrm{d}\mathbf{z} \\
&\quad - \langle \kappa_{ik}(\mathbf{x}) \{ \partial_{x_k} \partial_{x'_\ell} G(\mathbf{x}, \mathbf{x}') \} \kappa_{\ell j}(\mathbf{x}') \rangle, \qquad (4.15a) \\
\tilde{c}(\mathbf{x}, \mathbf{x}') &= \langle c(\mathbf{x}) \rangle \\
&\quad + s \int_{\Omega} \langle c(\mathbf{x}) G(\mathbf{x}, \mathbf{y}) w^{(1)}(\mathbf{y}) \rangle \mathrm{d}\mathbf{y} \int_{\Omega} \langle w^{(2)} G w^{(1)} \rangle^{-1}(\mathbf{y}, \mathbf{z}) \langle w^{(2)}(\mathbf{z}) G(\mathbf{z}, \mathbf{x}') c(\mathbf{x}') \rangle \mathrm{d}\mathbf{z} \\
&\quad - s \left\langle c(\mathbf{x}) G(\mathbf{x}, \mathbf{x}') c(\mathbf{x}') \right\rangle , \qquad (4.15b) \\
\tilde{\chi}_i(\mathbf{x}, \mathbf{x}') &= s \int_{\Omega} \langle \kappa_{ik}(\mathbf{x}) \partial_{x_k} G(\mathbf{x}, \mathbf{y}) w^{(1)}(\mathbf{y}) \rangle \mathrm{d}\mathbf{y} \int_{\Omega} \langle w^{(2)} G w^{(1)} \rangle^{-1}(\mathbf{y}, \mathbf{z}) \langle w^{(2)}(\mathbf{z}) \{ \partial_{x'_\ell} G(\mathbf{z}, \mathbf{x}') \} c(\mathbf{x}') \rangle \mathrm{d}\mathbf{z} \\
&\quad - s \langle \kappa_{ik}(\mathbf{x}) \{ \partial_{x_k} G(\mathbf{x}, \mathbf{x}') \} c(\mathbf{x}') \rangle, \qquad (4.15c) \\
\tilde{\xi}_j(\mathbf{x}, \mathbf{x}') &= \int_{\Omega} \langle c(\mathbf{x}) G(\mathbf{x}, \mathbf{y}) w^{(1)}(\mathbf{y}) \rangle \mathrm{d}\mathbf{y} \int_{\Omega} \langle w^{(2)} G w^{(1)} \rangle^{-1}(\mathbf{y}, \mathbf{z}) \langle w^{(2)}(\mathbf{z}) \{ \partial_{x'_\ell} G(\mathbf{z}, \mathbf{x}') \} \kappa_{lj}(\mathbf{x}') \rangle \mathrm{d}\mathbf{z} \\
&\quad - \langle c(\mathbf{x}) \{ \partial_{x_l} G(\mathbf{x}, \mathbf{x}') \} \kappa_{lj}(\mathbf{x}') \rangle. \qquad (4.15d)
\end{aligned}$$

5 Comments

Although Eq. (4.14) is formal in nature because it contains no prescription for calculating the Green's function of the random medium[vi], it reveals the general structure of the effective relations $\tilde{\mathsf{L}}$ and provides the following insights. Evidently, the effective constitutive equations are nonlocal in time and space, even though the microscopic equations are local and generally include nonzero cross-coupling terms $(\tilde{\boldsymbol{\chi}}, \tilde{\boldsymbol{\xi}})$, whose kernels are vector-valued. The cross-couplings form an adjoint pair as part of self-adjoint effective constitutive relations when $\boldsymbol{\kappa} = \boldsymbol{\kappa}^{\mathsf{T}}$ (so the composite is reciprocal) and $w^{(1)} = w^{(2)}$. Therefore, when the underlying composite is reciprocal, our effective model is reciprocal as well, as required [12, 15, 32]. The effective constitutive operator $\tilde{\mathsf{L}}$ (4.13) is reminiscent of equation (3.19) of Willis [8] for electromagnetics and elastodynamics, and its extension (without weighted mean) to electro-elastodynamics by Pernas-Salomón and Shmuel [14], see equation (15) therein. It is slightly more flexible than the former in that $w^{(1)}$ need not be the same as $w^{(2)}$. Notably, for the present problem, $\mathsf{B} \neq -(\mathsf{D}^{\mathsf{T}})^{\dagger}$ so both have to be explicit in $\tilde{\mathsf{L}}$. The result would remain applicable if the constitutive tensor L were full, i.e., the homogenization was of a medium made of thermally bianisotropic constituents.

[vi] A formulation employing a comparison linear medium which lends itself to approximation will be presented elsewhere.

The structure of $\tilde{\mathsf{L}}$ as evident in Eq. (4.15) motivates a different form of constitutive equations that includes the time rate of the effective temperature as a state variable, namely,

$$\begin{pmatrix} -\langle \mathbf{q} \rangle \\ \langle \theta_{\mathrm{R}} \eta \rangle \end{pmatrix} = \begin{pmatrix} \langle \boldsymbol{\kappa} \rangle & \mathbf{0} \\ \mathbf{0}^{\mathsf{T}} & \langle c \rangle \end{pmatrix} \begin{pmatrix} \langle \nabla w^{(2)} \theta \rangle - \boldsymbol{\zeta} \\ \langle w^{(2)} \theta \rangle \end{pmatrix} + \begin{pmatrix} \hat{\boldsymbol{\kappa}} & \check{\boldsymbol{\xi}} \\ \hat{\boldsymbol{\xi}} & \hat{c} \end{pmatrix} \begin{pmatrix} \langle \nabla w^{(2)} \theta \rangle - \boldsymbol{\zeta} \\ s \langle w^{(2)} \theta \rangle - \varphi \end{pmatrix}, \tag{5.1}$$

where $\check{\boldsymbol{\xi}} = \hat{\boldsymbol{\xi}}^{\dagger}$ when $\boldsymbol{\kappa}^{\mathsf{T}} = \boldsymbol{\kappa}$ and $w^{(1)} = w^{(2)}$. Spelling out this adjoint symmetry explicitly

$$\int_{\Omega} \left(\int_{\Omega} s \hat{\boldsymbol{\xi}}^{\dagger} (\mathbf{x}, \mathbf{x}') \, \theta (\mathbf{x}') \, \mathrm{d}\mathbf{x}' \right) \cdot \nabla \theta (\mathbf{x}) \, \mathrm{d}\mathbf{x} = \int_{\Omega} s \theta(\mathbf{x}) \left(\int_{\Omega} \hat{\boldsymbol{\xi}} (\mathbf{x}', \mathbf{x}) \cdot \nabla \theta (\mathbf{x}') \, \mathrm{d}\mathbf{x}' \right) \mathrm{d}\mathbf{x}. \tag{5.2}$$

The homogenized model delivers an effective equation for $\langle w^{(2)} \theta \rangle$ that may be fundamentally different from the equation for θ. Complete analysis admitting full nonlocal response is beyond the scope of the present work; here we recall several properties of its local approximation, which were noted in our companion paper [19] in the particular context of unweighted mean values. First, the local approximation of the effective equation for $\langle w^{(2)} \theta \rangle$ is a differential equation that is generally second-order in time as well as space, in contrast with the underlying diffusion equation for θ. Thus, the effective response consists of waves that travel at finite speed while still decaying, so long as $\hat{c} > 0$. If $\hat{c}$ were negative, the governing equation would be elliptic and not credible as the result of any time-dependent diffusive process. The one-dimensional local approximation of the effective equation contains also a mixed space-time derivative that depends on $\hat{\boldsymbol{\xi}} - \check{\boldsymbol{\xi}}$. In the self-adjoint case where $\check{\boldsymbol{\xi}} = \hat{\boldsymbol{\xi}}^{\dagger} = \hat{\boldsymbol{\xi}}$, the contribution of the bianisotropic terms to the effective differential equation vanishes; still, the adjoint pair changes the characteristic thermal impedance. In one-dimension under a time-harmonic heat source with frequency ω, the thermal impedance reads[vii]

$$Z_{\chi}^{\pm} = \frac{\theta^{\pm}}{q^{\pm}} = \left(\pm Z^{-1} - \tilde{\chi} \right)^{-1}, \tag{5.3}$$

where $Z^{-1} = k \tilde{\kappa}, k = \sqrt{cs/\kappa}$ is the wavenumber, $s = i\omega$ in this time-harmonic case, and the $\pm$ notation denotes quantities associated with forward- and backward disturbances (more details in Sec. 7). Thus, the bianisotropic terms capture direction-dependent impedance, similar to their role in wave systems [13, 16, 35].

We conclude this section commenting on the applicability of Eq. (4.14) to a periodic medium. This is carried out by regarding the composite as random through uncertainty in the position of any one reference point $\mathbf{y}$ in any one periodic cell. The Green's function for the random medium is then $G(\mathbf{x}, \mathbf{x}', \mathbf{y}) = G_0(\mathbf{x} - \mathbf{y}, \mathbf{x}' - \mathbf{y})$, where the random variable $\mathbf{y}$ is uniformly distributed over one cell, Ω_{p} say, fixed in space. This prescription was fully explained in Ref. [8] in the context of electromagnetics and elastodynamics and examples of its use were presented for periodic elastic laminates in Ref. [34]; and for piezoelectric laminates in Ref. [14].

[vii] Here we fix a typo in our companion paper, where the signs in the brackets were erroneously flipped.

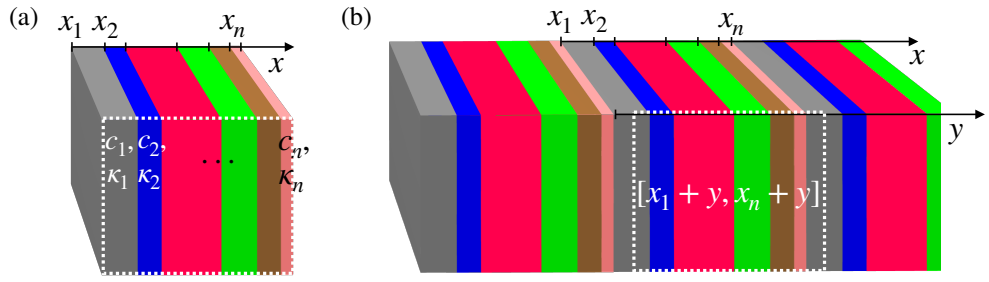

Figure 1: (a) A finite laminate occupying $x_1 < x < x_{n+1}$, composed of $n = 6$ isotropic laminae, with lamina r occupying $x_r < x < x_{r+1}$ and having conductivity κ_r and thermal capacity c_r. (b) Part of an infinite periodic composite using the laminate in (a) as its unit cell. An equivalent unit cell that yields the same periodic composite is denoted by the dashed frame over the interval $(x_1 + y, x_{n+1} + y)$, y being arbitrary.

6 Analysis and retrieval method in one-dimension

Consider a finite laminate occupying $x_1 < x < x_{n+1}$. It is composed of n isotropic laminae, with lamina r occupying $x_r < x < x_{r+1}$ and having conductivity κ_r and thermal capacity c_r (see Fig. 1a). Note first that, generically, a conventional medium with conductivity κ and heat capacity c admits solutions to Eq. (3.2) in the form

$$\mathsf{s}(x,t) := \begin{pmatrix} -q(x,t) \\ \theta(x,t) \end{pmatrix} = \begin{pmatrix} -e^{-kx}/Z & e^{kx}/Z \\ e^{-kx} & e^{kx} \end{pmatrix} \begin{pmatrix} a^+ \\ a^- \end{pmatrix} e^{st} =: \mathsf{Q}\,(x)\,\mathsf{a}\,e^{st}, \tag{6.1}$$

where k and Z were given in Sec. 5 (now with $\tilde{\xi} = 0$) and the coefficient a^+ (a^-) is the amplitude of the solution that decays in the positive (negative) direction. The spatial evolution of s can be written as

$$\mathsf{s}_{,x} = \begin{pmatrix} 0 & cs \\ 1/\kappa & 0 \end{pmatrix} \mathsf{s} =: \mathsf{M}\mathsf{s}. \tag{6.2}$$

So, the heat flux and temperature at 0 and x are related by

$$\mathsf{s}(x) = \mathsf{Q}\,(x)\,\mathsf{Q}^{-1}\,(0)\,\mathsf{s}(0) =: \mathsf{T}\mathsf{s}(0), \tag{6.3}$$

where

$$\mathsf{T} = e^{\mathsf{M}x} = \mathsf{I}\cosh kx + \mathsf{M}\frac{\sinh kx}{k} = \begin{pmatrix} \cosh kx & Z^{-1}\sinh kx \\ Z\sinh kx & \cosh kx \end{pmatrix} =: \begin{pmatrix} C & S/Z \\ ZS & C \end{pmatrix}, \tag{6.4}$$

is the transfer matrix. Note that $\mathsf{T}(x)\mathsf{T}(y) = \mathsf{T}(x+y)$, from which it follows that $\mathsf{T}^{-1}(x) = \mathsf{T}(-x)$. Also note that $\det \mathsf{T} = 1$, as required by reciprocity to ensure that the transmission is independent of the

incident direction. Now define T_r to be $\mathsf{T}(x_{r+1}-x_r)$ with κ and c taking the values κ_r and c_r respectively. It follows that

$$\mathsf{s}(x_n) = \mathsf{T}\mathsf{s}(x_1), \tag{6.5}$$

where T and M are no longer generic but are redefined to be

$$\mathsf{T} = \mathsf{T}_n\mathsf{T}_{n-1}...\mathsf{T}_1 = e^{M_n l_n}e^{M_{n-1}l_{n-1}}...e^{M_1 l_1}, \tag{6.6}$$

where $l_r = x_r - x_{r-1}$. Still $\det\mathsf{T} = 1$ since the determinant of the product equals the product of the determinants.

Suppose that the n-layered cell considered is embedded in an infinite medium with conductivity κ_0 and heat capacity c_0. Then, the most general freely propagating disturbance in the background medium is[viii]

$$\theta\,(x,t)\,e^{-st} = \begin{cases} a_{\mathrm{L}}^{-}e^{k_0(x-x_1)} + a_{\mathrm{L}}^{+}e^{-k_0(x-x_1)} & x \le x_1 \\ a_{\mathrm{R}}^{-}e^{k_0(x-x_{n+1})} + a_{\mathrm{R}}^{+}e^{-k_0(x-x_{n+1})} & x \ge x_{n+1} \end{cases}, k_0 = \sqrt{sc_0/\kappa_0}, \tag{6.7}$$

where k_0 has positive real part when s has positive real part. The coefficient a_{L}^{+} represents a disturbance incident from the left. It generates a reflected field with amplitude $a_{\mathrm{L}}^{-} = r_{\mathrm{L}}a_{\mathrm{L}}^{+}$, say, and a transmitted field $a_{\mathrm{R}}^{+} = t_{\mathrm{L}}a_{\mathrm{L}}^{+}$, where r_{L}, t_{L} are respectively the reflection and transmission coefficients for a disturbance incident from the left. Similarly, a disturbance incident from the right with amplitude a_{R}^{-}, generates a reflected field with amplitude $a_{\mathrm{R}}^{+} = r_{\mathrm{R}}a_{\mathrm{R}}^{-}$ and a transmitted disturbance with amplitude $a_{\mathrm{L}}^{-} = t_{\mathrm{R}}a_{\mathrm{R}}^{-}$. Now with the notation

$$\mathsf{a}_{\mathrm{L}} = \begin{pmatrix} a_{\mathrm{L}}^{+} \\ a_{\mathrm{L}}^{-} \end{pmatrix}, \quad \mathsf{a}_{\mathrm{R}} = \begin{pmatrix} a_{\mathrm{R}}^{+} \\ a_{\mathrm{R}}^{-} \end{pmatrix}, \tag{6.8}$$

these relations can be expressed in the form [36]

$$\mathsf{a}_{\mathrm{R}} = \mathsf{K}\mathsf{a}_{\mathrm{L}} \equiv \begin{pmatrix} t_{\mathrm{L}} - r_{\mathrm{R}}t_{\mathrm{R}}^{-1}r_{\mathrm{L}} & r_{\mathrm{R}}t_{\mathrm{R}}^{-1} \\ -r_{\mathrm{L}}t_{\mathrm{R}}^{-1} & t_{\mathrm{R}}^{-1} \end{pmatrix}\mathsf{a}_{\mathrm{L}}. \tag{6.9}$$

The components of the amplitude transfer matrix K are thus experimentally measurable from scattering experiments and their resultant reflection and transmission coefficients [37]. Retrieval methods aim at relating these measurements, or, equivalently, K, to the effective properties of the scatterer [16, 35, 38–40]. To develop a similar method here, we first recall that Eq. (6.1) implies

$$\mathsf{s}(x_1) = \mathsf{Q}_0(x_1)\mathsf{a}_{\mathrm{L}}, \tag{6.10}$$

where Q_0 takes the values k_0 and Z_0 (the same representation for s at $x = x_{n+1}$ applies, with a_{L} replaced by a_{R}). The continuity of q and θ at $x = x_1$ and $x = x_{n+1}$ requires that

$$\mathsf{Q}_0(x_{n+1})\mathsf{a}_{\mathrm{R}} = \mathsf{T}(\mathsf{Q}_0(x_1)\mathsf{a}_{\mathrm{L}}) \tag{6.11}$$

[viii] In our companion paper [19] $s = i\omega$ was adopted.

which, together with (6.9), gives

$$\mathsf{T} = \mathsf{Q}_0(x_{n+1})\mathsf{K}\mathsf{Q}_0^{-1}(x_1). \tag{6.12}$$

Note that $\det \mathsf{K} = t_L/t_R$, where reciprocity requires $t_L = t_R$, and so for K to be physically valid, it must satisfy $\det \mathsf{K} = 1$, as confirmed by the fact that $\det \mathsf{T} = 1$.

Relation (6.11) permits the experimental retrieval of T from scattering experiments. Heuristic methods of homogenization map this retrieved data to a fictitious homogeneous medium with some $\tilde{\mathsf{T}}$ that reproduces the same scattering response as the heterogeneous scatterer. The structure of T as follows from Eqs. (6.4) and (6.6) implies that, in the general case, this mapping to $\tilde{\kappa}$ and $\tilde{c}$ alone is not possible, and a third material parameter, $\tilde{\xi}$, is needed because generally T has three independent parameters ($r_{\mathrm{L}}, r_{\mathrm{R}}$ and $t_{\mathrm{L}} \equiv t_{\mathrm{R}}$).

Building on the conclusions of the exact homogenization method, we postulate a uniform medium governed by the local approximation of the bianisotropic constitutive equations,

$$-q = \tilde{\kappa}\theta_{,x} + \tilde{\chi}\theta, \quad \theta_{\mathrm{R}}\eta = \tilde{\xi}\theta_{,x} + \tilde{c}\theta, \tag{6.13}$$

an approximation which is valid when the thermal wavelength is much larger than the size of the medium. In the absence of sources, its corresponding energy equation is

$$\tilde{\kappa}\theta_{,xx} + (\tilde{\chi} - s\tilde{\xi})\theta_{,x} - s\tilde{c}\theta = 0. \tag{6.14}$$

The intention is to equate its transfer matrices to the corresponding matrices T and K of the original heterogeneous medium. To this end, we will calculate $\tilde{\mathsf{M}}$, starting by extracting $\theta_{,x}$ from the constitutive equation for q

$$\theta_{,x} = -\left(\frac{1}{\tilde{\kappa}}q + \frac{\tilde{\chi}}{\tilde{\kappa}}\theta\right); \tag{6.15}$$

and substituting this into the constitutive equation for the entropy to obtain

$$\theta_{\mathrm{R}}\eta = \left(\tilde{c} - \tilde{\xi}\frac{\tilde{\chi}}{\tilde{\kappa}}\right)\theta - \frac{\tilde{\xi}}{\tilde{\kappa}}q. \tag{6.16}$$

We can now use this expression in the energy equation to write $-q_{,x}$ as

$$-q_{,x} = s\theta_{\mathrm{R}}\eta = -s\left(\tilde{\xi}\frac{\tilde{\chi}}{\tilde{\kappa}} - \tilde{c}\right)\theta - s\frac{\tilde{\xi}}{\tilde{\kappa}}q. \tag{6.17}$$

So

$$\tilde{\mathsf{M}} = \tilde{\kappa}^{-1}\begin{pmatrix} s\tilde{\xi} & s\tilde{\kappa}\tilde{c} - s\tilde{\xi}\tilde{\chi} \\ 1 & -\tilde{\chi} \end{pmatrix}, \tag{6.18}$$

from which we obtain expressions for the effective properties in terms of the components of $\tilde{\mathsf{M}}$, as summarized in our companion paper[ix], namely,

$$\tilde{\kappa} = \frac{1}{\tilde{M}_{21}}, \quad \tilde{c} = -\frac{\det \tilde{M}}{s\, M_{21}}, \quad \tilde{\chi} = -\frac{\tilde{M}_{22}}{\tilde{M}_{21}}, \quad \tilde{\xi} = \frac{\tilde{M}_{11}}{s\tilde{M}_{21}}. \tag{6.19}$$

Since

$$\det\tilde{\mathsf{T}} = \det e^{\tilde{\mathsf{M}}x} = \det e^{\mathrm{tr}\,\tilde{\mathsf{M}}x}, \tag{6.20}$$

the requirement $\det \tilde{\mathsf{T}} = \det \mathsf{T} \equiv 1$ enforces traceless $\tilde{\mathsf{M}}$ and

$$\tilde{\chi} = s\tilde{\xi}, \tag{6.21}$$

reiterating the notion that the bianisotropic cross-couplings are an adjoint pair when the underlying medium is Hermitian. We can now apply Eq. (6.4) for the effective medium and obtain

$$\tilde{\mathsf{T}} = \begin{pmatrix} C + \tilde{\chi} ZS & (1 - \tilde{\chi}^2 Z^2) S/Z \\ ZS & C - \tilde{\chi} ZS \end{pmatrix}, \tag{6.22}$$

where now the argument of C and S is $\tilde{k}x$ with $\tilde{k} = (\tilde{c}s/\tilde{\kappa})^{1/2}$. Equivalently, result (6.22) can be obtained by observing that the general solution of Eq. (6.14) can be written as

$$\theta(x) = \theta_0 \cosh \tilde{k}x + A \sinh \tilde{k}x, \tag{6.23}$$

and correspondingly,

$$-q(x) = Z^{-1}(\theta_0 \sinh \tilde{k}x + A \cosh \tilde{k}x) + \tilde{\chi}\theta(x). \tag{6.24}$$

Then, if $q(0) = q_0$, this implies that $A = -Z(q_0 + \tilde{\chi}\theta_0)$ and Eq. (6.22) follows.

With x taking the value $l := x_{n+1} - x_1$, the matrix $\tilde{\mathsf{T}}$ is required to coincide with T, eventually providing

$$\tilde{\chi} = \frac{T_{11} - T_{22}}{2T_{21}}, \quad \tilde{\kappa} = \frac{Sl}{T_{21}\ln(C+S)}, \quad \tilde{c} = \frac{S\ln(C+S)}{sT_{21}l}, \text{ with } C = \frac{T_{11}+T_{22}}{2}, S = \sqrt{C^2-1}. \tag{6.25}$$

The calculation just summarized is equivalent to requiring that the scattering properties of the given composite layer, sandwiched between two conducting half-spaces, are reproduced if the composite is replaced by a layer of effective material with the properties as derived. We can therefore express the

[ix] Equation (8) in Ref. [19] is slightly different, there we used $i\omega$ instead of s, and defined the components of the state vector differently.

effective properties directly in terms of the measurable scattering coefficients, combining Eqs. (6.1), (6.9) and (6.12) gives

$$\tilde{\kappa} = Z_0^{-1}\,\frac{l}{\psi}\,\frac{\sqrt{\left(e^{2k_0 l}+t^2-r_{\mathrm{L}}r_{\mathrm{R}}\right)^2-4t^2e^{2k_0 l}}}{e^{2k_0 l}-t^2+r_L r_R+e^{k_0 l}\left(r_{\mathrm{L}}+r_{\mathrm{R}}\right)}, \tag{6.26a}$$

$$\tilde{c} = Z_0^{-1}\,\frac{\psi}{s\,l}\,\frac{\sqrt{\left(e^{2k_0 l}+t^2-r_{\mathrm{L}}r_{\mathrm{R}}\right)^2-4t^2e^{2k_0 l}}}{e^{2k_0 l}-t^2+r_L r_R+e^{k_0 l}\left(r_L+r_R\right)}, \tag{6.26b}$$

$$\tilde{\chi} = Z_0^{-1}\,\frac{e^{k_0 l}\left(r_{\mathrm{L}}-r_{\mathrm{R}}\right)}{e^{2k_0 l}-t^2+r_{\mathrm{L}}r_{\mathrm{R}}+e^{k_0 l}\left(r_{\mathrm{L}}+r_{\mathrm{R}}\right)} \equiv s\tilde{\xi}, \tag{6.26c}$$

where $\cosh\psi = [e^{k_0 l}+e^{-k_0 l}(t^2-r_{\mathrm{L}}r_{\mathrm{R}})]/2t$ and we used the center of the scatterer as the origin ($x_1 = -l/2, x_{n+1} = l/2$). Evidently, the bianisotropic terms capture asymmetry in the reflection properties of the scatterer, a manifestation of directional impedance.

Now consider an infinite periodic composite with the given composite layer as its unit cell (Fig. 1b). Floquet–Bloch waves of the form $f_{\mathrm{p}}(x)e^{k_{\mathrm{B}}x+st}$, where f_{p} is periodic with period l require that

$$\det(\mathsf{T}-e^{k_{\mathrm{B}}l}\mathsf{I}) = 0. \tag{6.27}$$

This reduces to the famous trace formula for waves in an n-component periodic laminate [41, 42],

$$2\cosh k_{\mathrm{B}}l = \operatorname{tr}\mathsf{T}, \tag{6.28}$$

because $\det\mathsf{T} = 1$. This is precisely the expression for C in Eq. (6.25). Thus, $k_{\mathrm{B}} = \tilde{k} = (\tilde{c}s/\tilde{\kappa})^{1/2}$ and is independent of $\tilde{\chi}$, as it must be if the periodic composite is replaced by the effective material as defined above.

There is, however, no need to identify the unit cell as the interval (x_1, x_{n+1}). It could equally be chosen as $(x_1+y, x_{n+1}+y)$ for any y, as denoted by the dashed frame in Fig. 1b.

7 Numerical examples

This Section provides numerical calculations for the effective properties of exemplary laminates, by applying the method in Sec. 6. The comprising materials of the analyzed laminates are summarized in Table 1, together with their parameters and physical units. For completeness, the physical units of $\tilde{\chi}$ and $\tilde{\xi}$ are respectively $\mathrm{W(m^2K)^{-1}}$ and $\mathrm{J(m^2K)^{-1}}$. The results will be presented in terms of dimensionless variables

$$\bar{\kappa} = \tilde{\kappa}/\kappa_0,\ \ \bar{c} = \tilde{c}/c_0,\ \ \bar{\chi} = \tilde{\chi}/\chi_0,\ \ \bar{\xi} = \tilde{\xi}/\xi_0,\ \ \bar{x} = x/l,\ \ \bar{\omega} = \omega c_0 l^2/\kappa_0, \tag{7.1}$$

Material	$\kappa\,[\mathrm{W\,m^{-1}\,K^{-1}}]$	$c\,[\mathrm{J\,m^{-3}\,K^{-1}}]$
SiO_2	1.38	1.65×10^6
Diamond	719	1.78×10^6
Copper	400	3.45×10^6

Table 1: Thermal conductivity and specific heat of the constituents employed in the calculations.

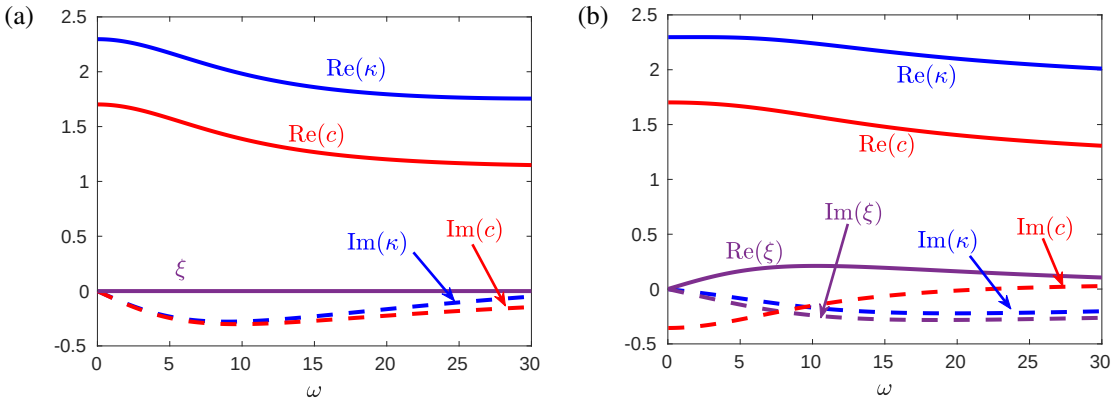

Figure 2: Effective properties of a bi-material laminate as functions of the normalized radian frequency ω. Real and imaginary parts of κ (blue), c (red) and ξ (purple) are shown in solid and dashed lines, respectively. (a) Symmetric arrangement. (b) Asymmetric arrangement.

where the period length l is measured in meters and

$$\chi_0 = \kappa_0/l, \quad \xi_0 = c_0 l. \tag{7.2}$$

The choice of κ_0 and c_0 has been made to respect the values shown in Table 1. Thus,

$$\kappa_0 = 1\ \mathrm{W(m\,K)^{-1}} \quad c_0 = 10^6\,\mathrm{J(m^3K)^{-1}}. \tag{7.3}$$

Fig. 2 relates to a laminate comprising a diamond layer sandwiched between two layers of silica. Fig. 2a corresponds to a symmetric arrangement in which the silica occupies the intervals $(0, 0.3)$ and $(0.7, 1)$ and the diamond occupies the middle layer, $(0.3, 0.7)$, while in Fig. 2b, the silica occupies $(0.15, 0.3)$ and $(0.7, 1.15)$. (The associated scattering configurations and interval identifications are shown in Fig. 3.) The plots in each case show the normalized effective properties κ (blue), c (red) and ξ (purple) as functions of normalized radian frequency ω.[x] Real parts are shown as solid lines and imaginary parts as dashed lines. The most noteworthy feature is that $\xi = 0$ in Fig. 2a, as it must be because the cell

[x]The bars over variables introduced above are now omitted.

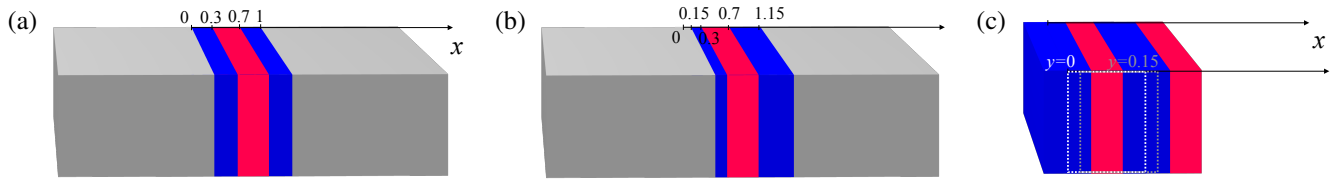

Figure 3: Scattering configurations corresponding to (a) the symmetric and (b) the asymmetric cells of Fig. 2. (c) Two interval identifications for these cells, indicated by the white (symmetric, $y = 0$) and gray (asymmetric, $y = 0.15$) frames.

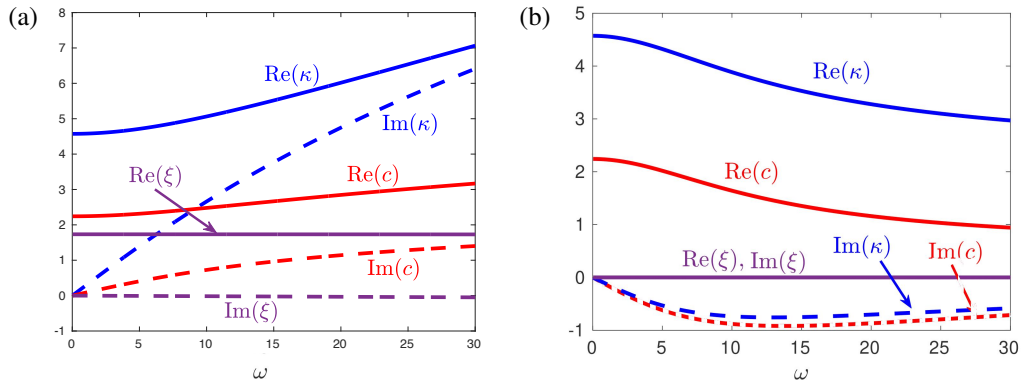

Figure 4: Effective properties of a tri-material laminate as functions of the normalized radian frequency ω. Legend as in Fig. 2. Panels (a) and (b) correspond respectively to the geometries considered in Figs. 2a and 2b, having the third layer replaced by copper.

geometry is symmetric about its midpoint and ξ is an odd function relative to a point of symmetry. It was remarked in our companion paper [19] that the gradient of the imaginary part of c with respect to ω was positive (for positive ω) for larger values of ω, suggesting a possible hyperbolic effective response as opposed to parabolic effective response; this is borne out in the plots.

Fig. 4 considers the same configurations as Fig. 2, having the third silica layer replaced by copper. (See Fig. 5 for the associated scattering configurations and interval identifications.) This cell displays physical asymmetry, regardless of where it is deemed to start. Now in Fig. 4a, ξ is found by computation to have real part virtually independent of ω and imaginary part close to zero, while Fig. 4b shows that ξ is virtually zero when the cell starts at $y = 0.15$.

Fig. 6 provides more detail of how the effective constants vary with the starting position y of the cell, at the arbitrarily-chosen dimensionless $\omega = 10$. Fig. 6a is for the cell composed of 60% silica and 40% diamond. It has reflection symmetry about $y = 0$ and $y = 0.5$ and Fig. 6a reflects this. Fig. 6b is for the tri-material laminate. There is no symmetry and it appears that there is little variation in κ and c, except when $y \in (0, 0.3)$, that is, when the front face is silica. However, ξ varies significantly throughout the full

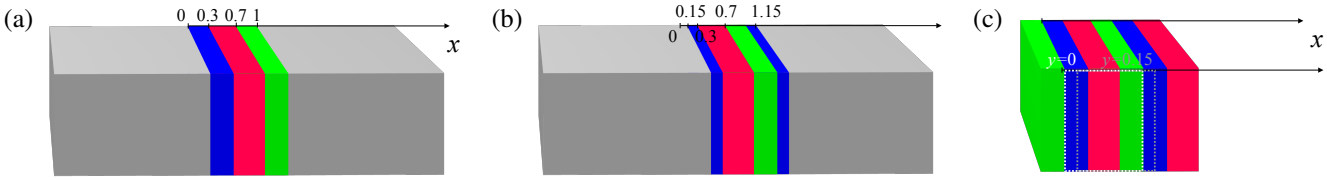

Figure 5: Scattering configurations corresponding to Fig. 4: (a) $y = 0$ and (b) $y = 0.15$, both extracted from the tri-material periodic laminate shown in (c). The two interval identifications are indicated by white and gray frames.

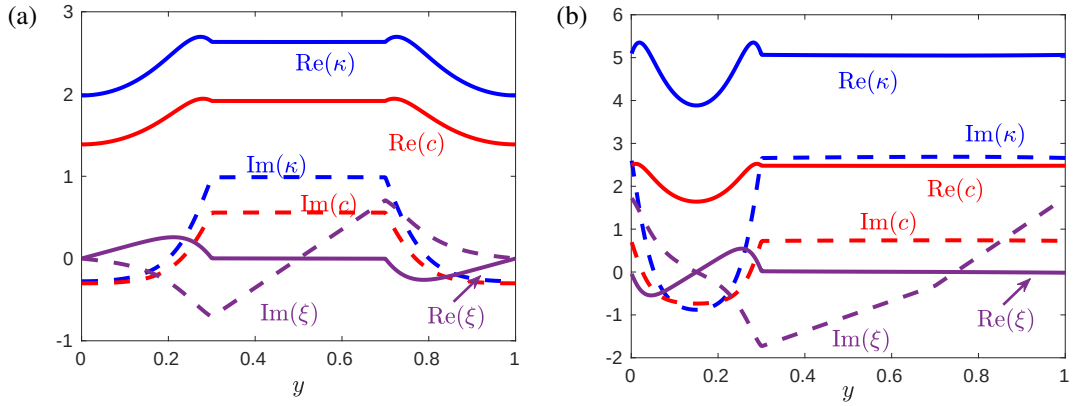

Figure 6: Effective properties at $\omega = 10$ of the (a) bi-material and (b) tri-material laminates as functions of y, for the cell $(y, y + 1)$. Legend as in Fig. 2.

range $(0, 1)$ of y, so that the end impedance remains sensitive to y.

As mentioned at the end of Section 6, a periodic laminate can support a rightward Floquet–Bloch disturbances of the form $\theta(x,t) = \theta_{\rm p}(x)e^{-k_{\rm B}x+st}$, with energy flux $q(x,t) = q_{\rm p}(x,t)e^{-k_{\rm B}x+st}$, where $\theta_{\rm p}(x)$ and $q_{\rm p}(x)$ are periodic with the period l of the medium[xi]. The periodic functions $\theta_{\rm p}$ and $q_{\rm p}$ depend on the details of the unit cell but the Floquet–Bloch complex wavenumber $k_{\rm B}$ is expressible as $k_{\rm B} = (cs/\kappa)^{1/2}$, where κ and c are effective properties of the unit cell; the constants ξ and $\chi = s\xi$ have no influence. The wave is time-harmonic if $s = i\omega$. The values of $\theta_{\rm p}$ and $q_{\rm p}$ at the left-hand end of the period depend on the choice of the interval that defines it but the Floquet–Bloch wavenumber $k_{\rm B}$ has to be independent of that choice, and the present calculations confirm this: the product $(\kappa c)^{1/2}$ is independent of y, even though κ and c vary with y, as shown in Fig. 6.

The thermal impedance at the left-hand end of the cell is obtained by noting that q satisfies Eq. (6.1) and $\theta_{,x} = -k_{\rm B}\theta$ for the right-traveling disturbance, so that

$$-q = (\chi - k_{\rm B}\kappa)\theta = s^{1/2}[s^{1/2}\xi - (c\kappa)^{1/2}]\theta. \tag{7.4}$$

[xi]Relative to the chosen dimensionless formulation, $l = 1$.

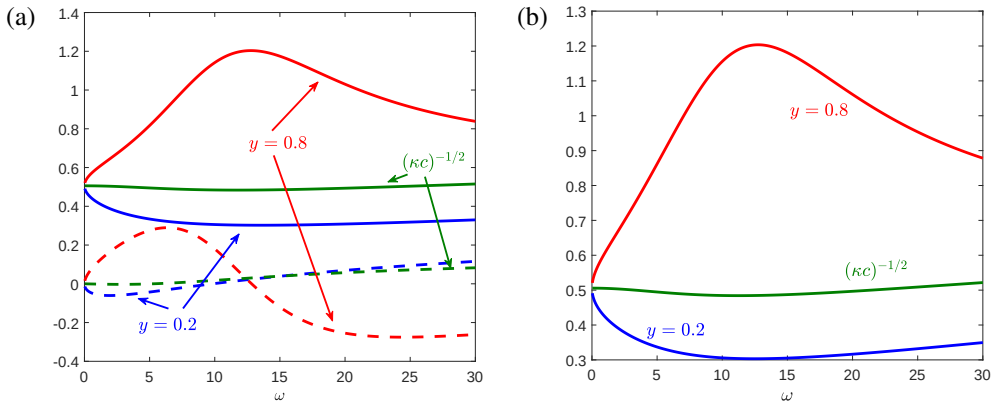

Figure 7: Normalized thermal impedances $\hat{Z}_\chi^+$ versus ω for the bi-material laminates when $y = 0.2$ (blue) and 0.8 (red). (a) Real and imaginary parts in solid and dashed curves (b) Absolute values. The term $(\kappa c)^{-1/2}$ is also shown in green.

It follows that the thermal impedance is

$$Z_\chi^+ = s^{-1/2}\hat{Z}_\chi^+, \tag{7.5}$$

where

$$\hat{Z}_\chi^+ = [(c\kappa)^{1/2} - s^{1/2}\xi]^{-1} = (Z^{-1} - s^{1/2}\xi)^{-1}. \tag{7.6}$$

A similar analysis for a left-traveling disturbance of dependence $e^{k_B x}$, for which $\theta_{,x} = k_B\theta$, results with

$$\hat{Z}^- = (-Z^{-1} - s^{1/2}\xi)^{-1}. \tag{7.7}$$

The difference between Eqs. (7.6) and (7.7) shows that the bianisotropic terms capture a directional part in the impedance. Fig. 7 shows dimensionless plots for $\hat{Z}_\chi^+$, for the bi-material laminates when $y = 0.2$ (blue curves) and 0.8 (red curves): Fig. 7a shows respectively the real and imaginary parts in solid and dashed curves, while Fig. 7b shows absolute values. The reason for the difference in impedances is that the excited right-traveling wave first encounters a layer of silica whose thickness is only 0.1 of the period when $y = 0.2$ whereas it first encounters a layer of thickness 0.5 of the period when $y = 0.8$. The curves for $y = 0.8$ can equally be regarded as plots of the thermal impedance for excitation at the right-hand side of a left-traveling wave in the cell occupying (0.2,1.2). In our companion paper [19] some results were shown for a cell of length $l = 50\,\text{nm}$. For this example, the physical ω is obtained by multiplying its dimensionless equivalent by $\kappa_0/(c_0 l^2) = 0.4 \times 10^9\ \text{s}^{-1}$, that is by 0.4 radians/ns. The dimensionless lengths chosen for the present figures do not correspond exactly to any used in our companion paper [19] but confirm the trends indicated there.

8 Summary

The advent of metamaterials has sparked interest in homogenization methods for identifying extraordinary effective responses in composite materials. A prominent exact method for waves was developed by Willis [6–8, 43], showing that effective responses become nonlocal in space and time and exhibit bianisotropy, even when the constituent responses are local and non-bianisotropic. Here, we have developed a homogenization framework that unifies diffusion and waves. As in wave systems, we find that the effective constitutive relations of heterogeneous conductors are nonlocal and include bianisotropic terms whose local part captures asymmetry-driven directional thermal impedance [13, 16, 35]. In contrast to wave systems, the effective diffusion equation may change character—from parabolic to hyperbolic. We expect the insights gained here, linking microstructural heterogeneities to anomalous macroscopic diffusion, to enable inverse design of thermal metamaterials [44–46]. In future work, we will extend this unified wave–diffusion homogenization framework to thermoelasticity with the premise of developing metamaterials exhibiting thermomomentum coupling.

Acknowledgments

G. S. thanks funding by the European Union (ERC, EXCEPTIONAL, Project No. 101045494). Funded by the European Union. Views and opinions expressed are, however, those of the author(s) only and do not necessarily reflect those of the European Union or the European Research Council Executive Agency. Neither the European Union nor the granting authority can be held responsible for them.

References

[1] Zvi Hashin. Analysis of composite materials—a survey. *Journal of Applied Mechanics*, 50(3):481–505, 1983.

[2] Graeme W Milton. *The theory of composites*. Cambridge University press, 2002.

[3] G Papanicolau, A Bensoussan, and J L Lions. *Asymptotic Analysis for Periodic Structures*. Studies in Mathematics and its Applications. Elsevier Science, 1978.

[4] T Antonakakis, R V Craster, and S Guenneau. Asymptotics for metamaterials and photonic crystals. *Proc. R. Soc. London A Math. Phys. Eng. Sci.*, 469(2152), 2013.

[5] H Nassar, Q.-C. He, and N Auffray. On asymptotic elastodynamic homogenization approaches for periodic media. *J. Mech. Phys. Solids*, 88:274–290, 2016.

[6] J R Willis. Variational principles for dynamic problems for inhomogeneous elastic media. *Wave Motion*, 3(1):1–11, 1981.

[7] J R Willis. Continuum Micromechanics. chapter Dynamics of Composites, pages 265–290. Springer-Verlag New York, Inc., New York, NY, USA, 1997.

[8] J R Willis. Effective constitutive relations for waves in composites and metamaterials. *Proc. R. Soc. London A Math. Phys. Eng. Sci.*, 467(2131):1865–1879, 2011.

[9] John R. Willis. The construction of effective relations for waves in a composite. *Comptes Rendus Mécanique*, 340(4):181 – 192, 2012. Recent Advances in Micromechanics of Materials.

[10] Shixu Meng and Bojan B Guzina. On the dynamic homogenization of periodic media: Willis' approach versus two-scale paradigm. *Proc. R. Soc. London A Math. Phys. Eng. Sci.*, 474(2213), 2018.

[11] H. Nassar, Q.-C. He, and N. Auffray. Willis elastodynamic homogenization theory revisited for periodic media. *Journal of the Mechanics and Physics of Solids*, 77:158–178, 2015.

[12] Michael B Muhlestein, Caleb F Sieck, Andrea Alù, and Michael R Haberman. Reciprocity, passivity and causality in Willis materials. *Proc. R. Soc. London A Math. Phys. Eng. Sci.*, 472(2194), 2016.

[13] Caleb F Sieck, Andrea Alù, and Michael R Haberman. Origins of Willis coupling and acoustic bianisotropy in acoustic metamaterials through source-driven homogenization. *Phys. Rev. B*, 96(10):104303, 2017.

[14] René Pernas-Salomón and Gal Shmuel. Symmetry breaking creates electro-momentum coupling in piezoelectric metamaterials. *Journal of the Mechanics and Physics of Solids*, 134:103770, 2020.

[15] René Pernas-Salomón and Gal Shmuel. Fundamental principles for generalized Willis metamaterials. *Phys. Rev. Applied*, 14:064005, Dec 2020.

[16] René Pernas-Salomón, Michael R. Haberman, Andrew N. Norris, and Gal Shmuel. The electromomentum effect in piezoelectric Willis scatterers. *Wave Motion*, page 102797, 2021.

[17] Alan Muhafra, Majd Kosta, Daniel Torrent, René Pernas-Salomón, and Gal Shmuel. Homogenization of piezoelectric planar Willis materials undergoing antiplane shear. *Wave Motion*, 108:102833, 2022.

[18] Kevin Muhafra, Michael R. Haberman, and Gal Shmuel. Discrete one-dimensional models for the electromomentum coupling. *Phys. Rev. Appl.*, 20:014042, Jul 2023.

[19] Gal Shmuel and John R. Willis. Thermally bianisotropic metamaterials induced by spatial asymmetry. *Phys. Rev. Lett.*, 135:116303, Sep 2025.

[20] Daniel Torrent, Olivier Poncelet, and Jean-Chirstophe Batsale. Nonreciprocal thermal material by spatiotemporal modulation. *Phys. Rev. Lett.*, 120:125501, Mar 2018.

[21] Liujun Xu, Guoqiang Xu, Jiaxin Li, Ying Li, Jiping Huang, and Cheng-Wei Qiu. Thermal Willis coupling in spatiotemporal diffusive metamaterials. *Phys. Rev. Lett.*, 129:155901, Oct 2022.

[22] Liujun Xu, Guoqiang Xu, Jiping Huang, and Cheng-Wei Qiu. Diffusive Fizeau drag in spatiotemporal thermal metamaterials. *Phys. Rev. Lett.*, 128:145901, Apr 2022.

[23] Chris Fietz and Gennady Shvets. Current-driven metamaterial homogenization. *Physica B: Condensed Matter*, 405(14):2930 – 2934, 2010. Proceedings of the Eighth International Conference on Electrical Transport and Optical Properties of Inhomogeneous Media.

[24] Andrea Alù. First-principles homogenization theory for periodic metamaterials. *Phys. Rev. B*, 84:075153, Aug 2011.

[25] G W Milton and J R Willis. On modifications of Newton's second law and linear continuum elastodynamics. *Proc. R. Soc. London A Math. Phys. Eng. Sci.*, 463(2079):855–880, 2007.

[26] J R Willis. Exact effective relations for dynamics of a laminated body. *Mech. Mater.*, 41(4):385–393, 2009.

[27] W. Kaminski. Hyperbolic heat conduction equation for materials with a nonhomogeneous inner structure. *Journal of Heat Transfer*, 112(3):555–560, 08 1990.

[28] S. L. Sobolev. Heat conduction equation for systems with an inhomogeneous internal structure. *Journal of Engineering Physics and Thermophysics*, 66(4):436–440, 1994.

[29] K. Mitra, S. Kumar, A. Vedavarz, and M. K. Moallemi. Experimental evidence of hyperbolic heat conduction in processed meat. *Journal of Heat Transfer*, 117(3):568–573, August 1995.

[30] Carlo Cattaneo. Sulla conduzione del calore. *Atti Sem. Mat. Fis. Univ. Modena*, 3:83–101, 1948.

[31] Gianfranco Capriz, Krzysztof Wilmanski, and Paolo Maria Mariano. Exact and approximate Maxwell-Cattaneo-type descriptions of heat conduction: A comparative analysis. *International Journal of Heat and Mass Transfer*, 175:121362, 2021.

[32] Andrea Alù. Restoring the physical meaning of metamaterial constitutive parameters. *Phys. Rev. B*, 83:081102, Feb 2011.

[33] Graeme W Milton. New metamaterials with macroscopic behavior outside that of continuum elastodynamics. *New Journal of Physics*, 9(10):359–359, oct 2007.

[34] J.R. Willis. A comparison of two formulations for effective relations for waves in a composite. *Mechanics of Materials*, 47:51 – 60, 2012.

[35] Michael B. Muhlestein, Caleb F. Sieck, Preston S. Wilson, and Michael R. Haberman. Experimental evidence of Willis coupling in a one-dimensional effective material element. *Nature Communications*, 8:15625 EP –, 06 2017.

[36] R Pérez-Álvarez, René Pernas-Salomón, and VR Velasco. Relations between transfer matrices and numerical stability analysis to avoid the ω problem. *SIAM Journal on Applied Mathematics*, 75(4):1403–1423, 2015.

[37] C. A. Bennett and R. R. Patty. Thermal wave interferometry: a potential application of the photoacoustic effect. *Appl. Opt.*, 21(1):49–54, Jan 1982.

[38] D. R. Smith, S. Schultz, P. Markoš, and C. M. Soukoulis. Determination of effective permittivity and permeability of metamaterials from reflection and transmission coefficients. *Phys. Rev. B*, 65:195104, Apr 2002.

[39] Vladimir Fokin, Muralidhar Ambati, Cheng Sun, and Xiang Zhang. Method for retrieving effective properties of locally resonant acoustic metamaterials. *Phys. Rev. B*, 76(14):144302, 2007.

[40] Xiaoshi Su and Andrew N. Norris. Retrieval method for the bianisotropic polarizability tensor of Willis acoustic scatterers. *Phys. Rev. B*, 98:174305, Nov 2018.

[41] Mahito Kohmoto, Leo P Kadanoff, and Chao Tang. Localization Problem in One Dimension: Mapping and Escape. *Phys. Rev. Lett.*, 50(23):1870–1872, 1983.

[42] John Lekner. Light in periodically stratified media. *J. Opt. Soc. Am. A*, 11(11):2892–2899, 1994.

[43] J R Willis. The nonlocal influence of density variations in a composite. *Int. J. Solids Struct.*, 21(7):805–817, 1985.

[44] Ying Li, Wei Li, Tiancheng Han, Xu Zheng, Jiaxin Li, Baowen Li, Shanhui Fan, and Cheng-Wei Qiu. Transforming heat transfer with thermal metamaterials and devices. *Nature Reviews Materials*, 6(6):488–507, 2021.

[45] Zeren Zhang, Liujun Xu, Teng Qu, Min Lei, Zhi-Kang Lin, Xiaoping Ouyang, Jian-Hua Jiang, and Jiping Huang. Diffusion metamaterials. *Nature Reviews Physics*, 5(4):218–235, 2023.

[46] Muamer Kadic, Tiemo Bückmann, Robert Schittny, and Martin Wegener. Metamaterials beyond electromagnetism. *Reports on Progress in Physics*, 76(12):126501, 2013.